Inorganic Chemistry

Article

pubs.acs.org/IC

Emissive Osmium(II) Complexes Supported by N-Heterocyclic Carbene-based C^C^C-Pincer Ligands and Aromatic Diimines

Lai-Hon Chung, Siu-Chung Chan, Wing-Chun Lee, and Chun-Yuen Wong*

Department of Biology and Chemistry, City University of Hong Kong, Tat Chee Avenue, Kowloon, Hong Kong SAR, People's Republic of China

Supporting Information

ABSTRACT: Osmium(II) complexes containing N-heterocyclic carbene (NHC)-based pincer ligand 1,3-bis(1-methylimidazolin-2-ylidene)phenyl anion (C^{1}^C^C^{1}) or 1,3-bis(3-methylbenzimidazolin-2-ylidene)phenyl anion (C^{2}^C^C^{2}) and aromatic diimine (2,2′-bipyridine (bpy), 1,10-phenanthroline (phen), or 4,4′-diphenyl-2,2′-bipyridine (Ph_2bpy)) in the form of [Os(C^C^C)(N^N)(CO)]$^+$ have been prepared. Crystal structures for these complexes show that the Os−C_{NHC} bonds are essentially single (Os−C_{NHC} distances = 2.079(5)−2.103(7) Å). Spectroscopic comparisons and time-dependent density functional theory (TD-DFT) calculations suggest that the lowest-energy electronic transition associated with these complexes (λ_{max} = 493−536 nm, ε_{max} = (5−10) × 10^3 dm^3 mol^{-1} cm^{-1}, solvent = CH_3CN) originate from a $d_\pi(Os^{II}) \rightarrow \pi^*$(N^N) metal-to-ligand charge transfer transition, where the $d_\pi(Os^{II})$ and π^*(N^N) levels contain significant contribution from the C^C^C ligands. All these complexes are emissive in the red-spectral region (674−731 nm) with quantum yields of 10^{-4}−10^{-2} and emission lifetimes of around 1−6 μs. Transient absorption spectroscopy and spectroelectrochemical measurements have also been used to probe the nature of the emissive excited-states. Overall, this joint experimental and theoretical investigation reveals that the C^C^C ligands can be used to modulate the photophysical properties of a [Os(N^N)] core via the formation of the hybrid [Os + C^C^C] frontier orbitals.

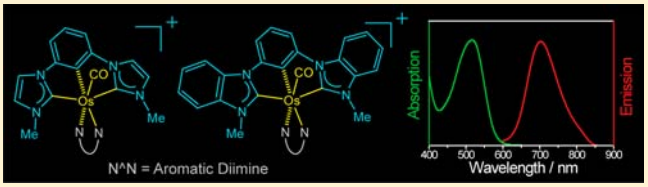

INTRODUCTION

Polypyridyl ruthenium(II) complexes and other d^6-transition metal counterparts represent an important class of functional molecular material.[1−13] Their rich photophysics and photochemistry originating from the triplet [d_π(M) → π^*-(polypyridyl)] metal-to-ligand charge transfer (^{3}MLCT) excited-state capture considerable attention because of their extensive applications in solar energy harvesting,[11,14,15] organic light emitting devices (OLEDs),[16,17] photochemistry,[11,18] and biolabeling reagents.[19] On the other hand, polypyridyl osmium(II) complexes also receive great interest regarding the design of functional optical materials on the ground that osmium is a heavier analogue of ruthenium.[13,16,17c,d]

For polypyridyl d^6-transition metal luminophores, it has been widely accepted that the presence of a close-lying thermally populated metal-centered ^{3}dd excited state (also known as triplet metal-centered state (^{3}MC) or triplet ligand-field state (^{3}LF)) serves as an efficient nonradiative deactivation pathway for the emissive d_π(M) → π^*(polypyridyl) ^{3}MLCT excited-state.[3] One of the promising approaches to enhance the emission of these complexes is to depopulate the ^{3}dd excited states by using stronger σ-donating ligands.[3,20−22] Practically this can be achieved by substituting the polypyridyl ligands by cyclometalating ligands.[11,14d,23,24]

On the other hand, N-heterocyclic carbenes (NHCs), a class of strong σ-donors, are widely used in metal-mediated catalysis but rarely employed as cyclometalating ligands to manipulate/modulate the photophysical properties associated with the derived complexes. NHCs were first isolated as stable compounds by Arduengo and co-workers in 1991.[25] Since this discovery, intensive investigations on NHCs and the derived metal complexes have been continuing but these studies centralize on the development of new generation of catalytic reagents.[26] NHC-based catalysts at the moment are widely employed to replace phosphine-based catalysts with reasons that NHCs are better electron-donors and can withstand a broader range of reaction conditions.[27] In fact, NHC-containing metal complexes with decent emissive properties have been reported. For example, successful improvement on emission behavior of Ir(III) complexes by manipulating NHCs as hard donors have been reported.[28] Several emissive NHC-containing Cu, Ag, and Au complexes have been prepared, in which the NHCs facilitate the metal−metal interaction-induced emissions.[29] Some emissive Pt−NHC complexes exhibit solvatochromatic photoluminescent behavior, and can be used as dopants in OLED.[30] Meanwhile, photophysical studies on Ru(II)− and Os(II)−NHC complexes are sparse. The most relevant study was performed on Ru(II) complexes bearing the bidentate and tridentate NHC ligands 3-methyl-1-(2-pyridyl)imidazol-2-ylidene and 2,6-bis(1-methylimidazolin-2-ylidene)pyridine.[31] Among them, the tridentate analogues show extensively long emission lifetime in

Received: December 20, 2011
Published: August 8, 2012

dx.doi.org/10.1021/ic202726g | Inorg. Chem. 2012, 51, 8693−8703

Scheme 1

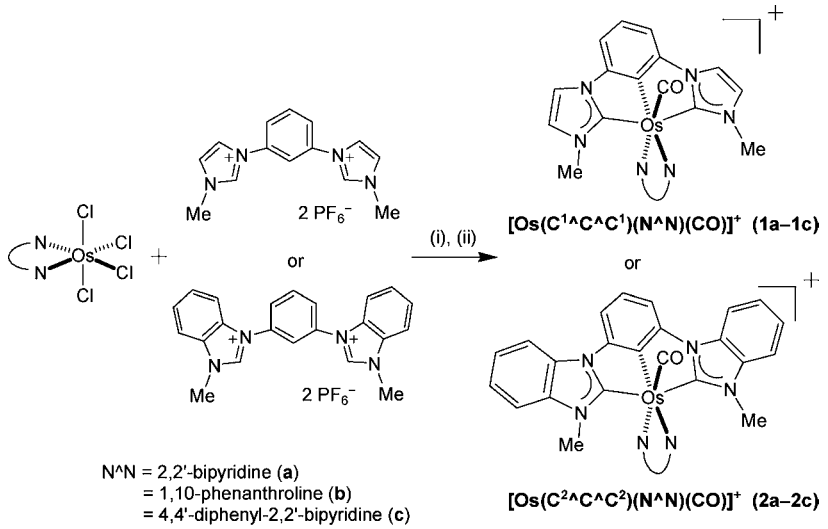

(i) Ethylene glycol, reflux; (ii) Zn/CH_3CN, reflux.

water and demonstrate some efficiencies in dye-sensitized solar-cell.[31b]

We have previously initiated a program to develop organometallic Ru(II)−diimine and related luminophores,[32] and have recently performed spectroscopic and theoretical investigations on Os(II)−NHC complexes in the form of $[Os(C^N^C)(N^N)Cl]^+$ where C^N^C are 2,6-bis-(alkylimidazolin-2-ylidene)pyridine or 2,6-bis(3-butylbenzimi-dazolin-2-ylidene)pyridine, and N^N are aromatic diimines.[33] In this work, a series of Os(II) complexes with the formula $[Os(C^C^C)(N^N)(CO)]^+$ have been prepared where C^C^C are 1,3-bis(1-methylimidazolin-2-ylidene)phenyl anion or 1,3-bis(3-methylbenzimidazolin-2-ylidene)phenyl anion, which can be viewed as anionic analogues of C^N^C. Although the $[Os(C^N^C)(N^N)Cl]^+$ complexes are not emissive in the visible region, the $[Os(C^C^C)(N^N)(CO)]^+$ complexes in this work are emissive in the red-spectral region with extraordinarily longer emission lifetime (around 1−6 μs at room temperature in fluid) than their classical diimine congeners such as $[Os(bpy)_3]^{2+}$ (60 ns) and $[Os(phen)_3]^{2+}$ (262 ns).[34] Supported by both experimental data and theoretical studies, the emissive excited-state originates from a $d_\pi(Os^{II}) \rightarrow \pi^*(N^N)$ MLCT transition. Importantly, these $d_\pi(Os^{II})$ and $\pi^*(N^N)$ levels contain significant contribution from the C^C^C ligands, and this reveals that the C^C^C ligands would not only act as point charge/spectator ligands, but can also be involved in the emissive excited-state to modify the photophysical properties of [Os(N^N)]-containing luminophores.

RESULTS AND DISCUSSION

Synthesis and Characterization. Reaction of $[Os(N^N)Cl_4]$ with the benzene-bridged bisimidazolium or bisbenzimidazolium hexafluorophosphate (precursors for $C^1{\wedge}C^{\wedge}C^1$ and $C^2{\wedge}C^{\wedge}C^2$ respectively) in refluxing ethylene glycol followed by reduction by Zn granules in refluxing CH_3CN afforded the C^C^C-pincer-ligated complexes $[Os(C^C^C)(N^N)(CO)]^+$ (**1**−**2**, Scheme 1). Instead of chloride, carbonyl group attaches to the Os center as an ancillary ligand, and this is likely due to the reductive carbonylation by ethylene glycol.[35] Interestingly, reaction of $[Os(N^N)Cl_4]$ with the pyridine-bridged bisimidazolium or bisbenzimidazolium hexafluorophosphate (precursors for C^N^C) under similar reaction conditions only gave the chloride-ligated complexes in the form of $[Os(C^N^C)(N^N)Cl]^+$.[33] Attempts to prepare $[Os(N^N)Cl_4]$ where N^N are dipyrido-[3,2-f:2′,3′-h]-quinoxaline, dipyrido-[3,2-a:2′,3′-c]-phenazine, 5,5′-dibromo-2,2′-bipyridine, 4,4′-dimethyl-2,2′-bi-pyridine, and 4,4′-dimethoxy-2,2′-bipyridine according to the method described by Buckingham et al.[36] and a modified procedure[33] failed, and therefore the corresponding $[Os(C^C^C)(N^N)(CO)]^+$ were not obtained. Both the ^1H and ^{13}C NMR spectra of **1**−**2** signify that the complexes possess a pseudoplane of symmetry in solution on the NMR time scale at room temperature. The ^{13}C NMR signals at 172.7−185.3 ppm for **1**−**2** are typical for metalated N-heterocyclic carbenes on Os(II) complexes.[33,37] The $\nu_{C\equiv O}$ stretching frequencies for **1** are 1906−1910 cm^{-1}, whereas those for **2** are 1924−1927 cm^{-1}, suggesting that (1) the Os center is not very sensitive to the change of N^N, and (2) increasing the conjugation of NHC by changing imidazolin-2-ylidene to benzimidazolin-2-ylidene on the C^C^C decreases its electron donating ability. Importantly, the Os−C bond distances, planarity and bite angles for C^C^C in **1a** and **2a** determined by X-ray crystallography are essentially the same (see discussion below), and this reveals that the difference in the donating ability between $C^1{\wedge}C^{\wedge}C^1$ and $C^2{\wedge}C^{\wedge}C^2$ is likely due to electronic factor.

The molecular structures of **1a**, **1b**, and **2a** have been determined by X-ray crystallography. Perspective views of **1a** and **2a** are depicted in Figure 1. Selected bond distances and angles are summarized in Table 1. In each case, the Os atom adopts a distorted octahedral geometry, with the C^C^C coordinating meridionally in an almost planar configuration. The bite angles for the C^C^C are 152.4(3)−153.0(2)°. The $Os-C_{NHC}$ distances (2.079(5)−2.103(7) Å) are slightly longer than the $Os-C_{Ph}$ distances (2.011(7)−2.029(7) Å), but all these are of single bond character despite that Os(II) is a good π-base; the $Os-C_{CO}$ distances are appreciably shorter (1.836(8)−1.879(5) Å) and this signifies the presence of Os(II) to CO π-backbonding interaction. Overall, the structural parameters of the coordination sphere around the Os center are not sensitive to the change of C^C^C (from $C^1{\wedge}C^{\wedge}C^1$ to

dx.doi.org/10.1021/ic202726g | Inorg. Chem. 2012, 51, 8693−8703

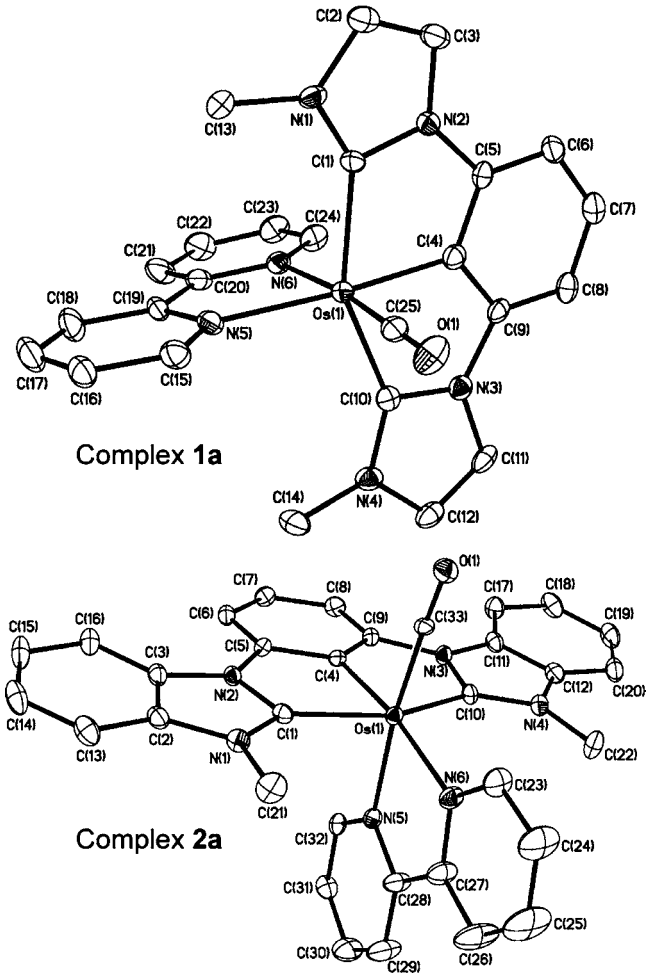

Figure 1. Perspective views of **1a** and **2a**. Hydrogen atoms are omitted for clarity. Thermal ellipsoids are at the 30% probability level.

Table 1. Selected Bond Lengths (Å) and Angles (deg) for 1a, 1b, and 2a

complex	1a	1b	2a
Os−C_{NHC}	2.093(6), 2.095(7)	2.088(7), 2.103(7)	2.079(5), 2.080(5)
Os−C_{Ph}	2.029(7)	2.011(7)	2.024(6)
Os−C_{CO}	1.859(8)	1.836(8)	1.879(5)
Os−N	2.138(5), 2.140(5)	2.142(6), 2.141(6)	2.123(5), 2.120(5)
C−O	1.162(9)	1.162(9)	1.125(7)
C_{NHC}−Os−C_{Ph}	75.6(3), 76.8(3)	76.1(3), 76.8(3)	76.4(2), 76.7(2)
∠Ph/NHC[a]	5.97, 7.05	2.80, 4.31	5.85, 6.25
∠NHC/NHC[b]	13.00	6.09	2.30

[a]The angle between the mean plane of the phenyl ring and the mean plane constructed by the imidazolin-2-ylidene or benzimidazolin-2-ylidene moiety. [b]The angle between the mean planes of the imidazolin-2-ylidene or benzimidazolin-2-ylidene moiety (mean planes are calculated from all non-hydrogen atoms on the moiety).

C^2^C^C^2) and N^N (from bpy to phen). It is noted that the bite angles for the NHC-pincer ligand and Os−C_{NHC} bond distances in this work are very close to those in the 2,6-bis(methylimidazolin-2-ylidene)pyridine (C^N^C)-ligated analogue $[Os(C^N^C)(bpy)Cl]^+$ (153.45(15)° and 2.042(4)−2.059(4) Å respectively),[33] regardless of the difference in the charge between C^C^C and C^N^C.

UV−Visible Absorption and Theoretical Studies. The UV−visible spectral data of the complexes are summarized in Table 2, and selected absorption spectra are depicted in Figure

Table 2. UV−Visible Absorption Data

complex	λ_{max}/nm (ε_{max}/dm^3 mol^{-1} cm^{-1})
	solvent = CH_3CN
1a	225 (42030), 247 (sh, 28280), 255 (sh, 22750), 287 (24910), 303 (sh, 16910), 371 (5660), 516 (5250)
1b	222 (58110), 265 (33820), 293 (sh, 12990), 323 (sh, 5470), 345 (sh, 3160), 506 (6420)
1c	224 (48400), 258 (72470), 303 (sh, 42150), 401 (12310), 536 (9350)
2a	211 (55340), 247 (55700), 275 (sh, 38900), 286 (41600), 303 (sh, 23760), 330 (sh, 13900), 374 (sh, 5600), 501 (5370)
2b	247 (52280), 271 (sh, 47850), 285 (sh, 36830), 316 (15450), 397 (sh, 3720), 493 (6600)
2c	249 (sh, 68970), 261 (sh, 63830), 289 (48900), 317 (sh, 32300), 390 (12430), 520 (9630)
	solvent = CH_2Cl_2
1a	256 (sh, 25510), 290 (28730), 322 (sh, 7530), 380 (6360), 535 (5820)
1b	266 (39820), 295 (sh, 14570), 321 (sh, 6840), 349 (3550), 525 (7870)
1c	257 (55500), 270 (sh, 43400), 306 (36710), 410 (14480), 520 (sh, 8890), 557 (10840)
2a	249 (61300), 288 (48930), 308 (sh, 22140), 329 (sh, 15260), 377 (7160), 524 (6280)
2b	250 (57620), 264 (57250), 287 (sh, 41640), 324 (sh, 16210), 396 (4300), 514 (7890)
2c	251 (sh, 67300), 263 (sh, 63630), 288 (49800), 316 (sh, 32970), 402 (13500), 507 (sh, 8700), 543 (10130)
	solvent = $(CH_3)_2CO$
1a	375 (6150), 522 (5920)
1b	345 (3740), 512 (7500)
1c	404 (12250), 542 (9250)
2a	368 (sh, 6270), 504 (5600)
2b	390 (sh, 3300), 496 (6330)
2c	392 (12530), 523 (9730)
	solvent = $(CH_3)_2SO$
1a	291 (26290), 305 (sh, 20790), 374 (6180), 519 (5880)
1b	269 (37510), 348 (sh, 3570), 511 (7180)
1c	309 (35670), 406 (13870), 540 (11030)
2a	279 (sh, 40500), 288 (42200), 305 (27130), 332 (sh, 14700), 371 (sh, 6130), 500 (5630)
2b	273 (sh, 56970), 288 (sh, 43570), 321 (sh, 17330), 493 (7710)
2c	288 (49630), 322 (sh, 32900), 393 (12270), 521 (9900)

2. All these complexes exhibit intense, high-energy absorption at $\lambda \leq 330$ nm ($\varepsilon_{max} \geq 10^4$ dm^3 mol^{-1} cm^{-1}, solvent = CH_3CN), and moderately intense bands at $\lambda > 330$ nm (ε_{max} = (5−10) × 10^3 dm^3 mol^{-1} cm^{-1}, solvent = CH_3CN) with tailing up to 650 nm as their lowest-energy electronic transition. The nature of these transitions are interesting and worth discussion. In the literature, Ru(II) and Os(II) complexes bearing polypyridine ligands feature two types of characteristic absorption bands: highly intense absorptions in the UV region attributed to the polypyridine intraligand (IL) $\pi \rightarrow \pi^*$ transitions, and moderately intense absorptions in the visible region, which are ascribed to $d_\pi(Ru^{II}/Os^{II}) \rightarrow \pi^*$(polypyridine) metal-to-ligand charge transfer (MLCT) transitions.[5−8,11,14d] Regarding complexes **1**−**2**, although one would expect the existence of both the $d_\pi(Os^{II}) \rightarrow \pi^*$(N^N) and $d_\pi(Os^{II}) \rightarrow \pi^*$(C^C^C) MLCT transitions at $\lambda > 330$ nm, it is noted that the nature of the transitions in this region cannot be simply assigned as a mixture of these transitions, arguments are as

dx.doi.org/10.1021/ic202726g | Inorg. Chem. 2012, 51, 8693−8703

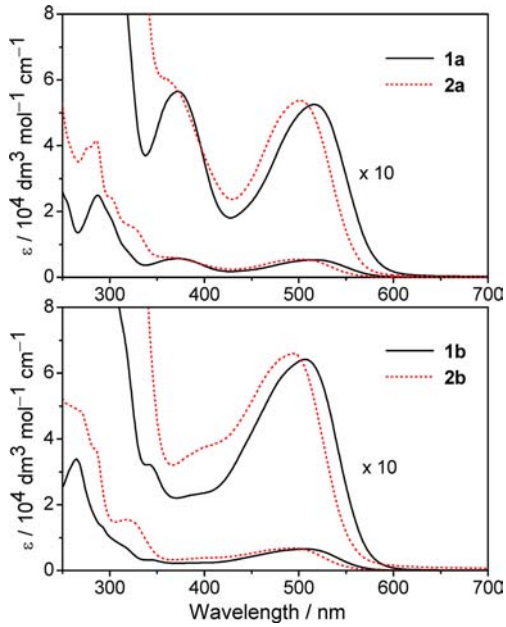

Figure 2. UV−visible absorption spectra of selected complexes in CH_3CN at 298 K.

follows: (1) The absorption profiles for **1a** and **1b** (and for **2a** and **2b**) are notably different at λ = 330−420 nm, and are comparable at λ > 420 nm. Since **1a**(**2a**) differs from **1b**(**2b**) by a N^N unit, the absorption bands at λ = 330−420 nm seems assignable to be the $d_\pi(Os^{II}) \rightarrow \pi^*(N^\wedge N)$ MLCT transition whereas those at λ > 420 nm to be the $d_\pi(Os^{II}) \rightarrow \pi^*(C^\wedge C^\wedge C)$ MLCT transition, but such assignments contradict the following argument. (2) C^C^C in **2a** is more conjugated than that in **1a** and hence is expected to possess a lower-lying π^* orbital. However, no red-shift of the lowest-energy absorption band is observed in **2a** when compared with that in **1a**, suggesting that the absorption at λ > 420 nm should not be attributed to $d_\pi(Os^{II}) \rightarrow \pi^*(C^\wedge C^\wedge C)$ MLCT transition. The comparisons between the **1b**/**2b** and **1c**/**2c** pairs also support this argument. (3) The $d_\pi(Os^{II}) \rightarrow \pi^*(N^\wedge N)$ MLCT transitions are expected to be very similar in energy for N^N = bpy or phen, and a red-shift is expected when N^N with lower π^* level (e.g., Ph_2bpy) is used. In this work, the similarity in the absorption profiles at λ > 420 nm between **1a** and **1b** (and between **2a** and **2b**), together with the red-shift in energy for **1c** (**2c**) compared with **1a** (**2a**), suggest that the absorption in this region to be the $d_\pi(Os^{II}) \rightarrow \pi^*(N^\wedge N)$ MLCT transition. Interestingly, complexes in the form of $[Os(C^\wedge N^\wedge C)(N^\wedge N)Cl]^+$ also exhibit moderately intense bands at λ > 320 nm ($\varepsilon_{max} \approx 10^3$−$10^4$ dm^3 mol^{-1} cm^{-1}) with absorption tails up to 800 nm;[33] these absorption profiles are susceptible to the change of N^N, and the tailings are not sensitive to the change of the conjugation on the C^N^C moiety, suggesting that the lowest-energy absorption for $[Os(C^\wedge N^\wedge C)(N^\wedge N)Cl]^+$ contains some $d_\pi(Os^{II}) \rightarrow \pi^*(N^\wedge N)$ MLCT character.

To rationalize the nature of electronic transitions associated with these complexes, time-dependent density functional theory (TD-DFT) calculations have been performed on **1**−**2** (with C_s symmetry imposed). The usage of C_s symmetry can provide a simple model to interpret the nature of the molecular orbitals, and it is justified because all the complexes possess a pseudo plane of symmetry in solution on the NMR time scale. The M06 functional[38] developed by Truhlar and Zhao has been used in these calculations. A TD-DFT calculation using the B3LYP functional[39] has also been performed on **1a** (with the M06 optimized geometry) for comparison, and the result is in agreement with the one using M06 functional. For the ease of discussion, only the results obtained by M06 functional would be discussed below. The conductor polarizable continuum model (CPCM)[40] has also been applied to account for solvent effects upon the electronic transition. Calculated excitation energies, oscillator strengths, and absorption spectra constructed by convolution of these calculated transitions with Gaussian functions, are depicted in Figure 3. The profiles of the convoluted absorption spectra resemble to those observed experimentally: the calculated spectra for **1a** and **2a** show

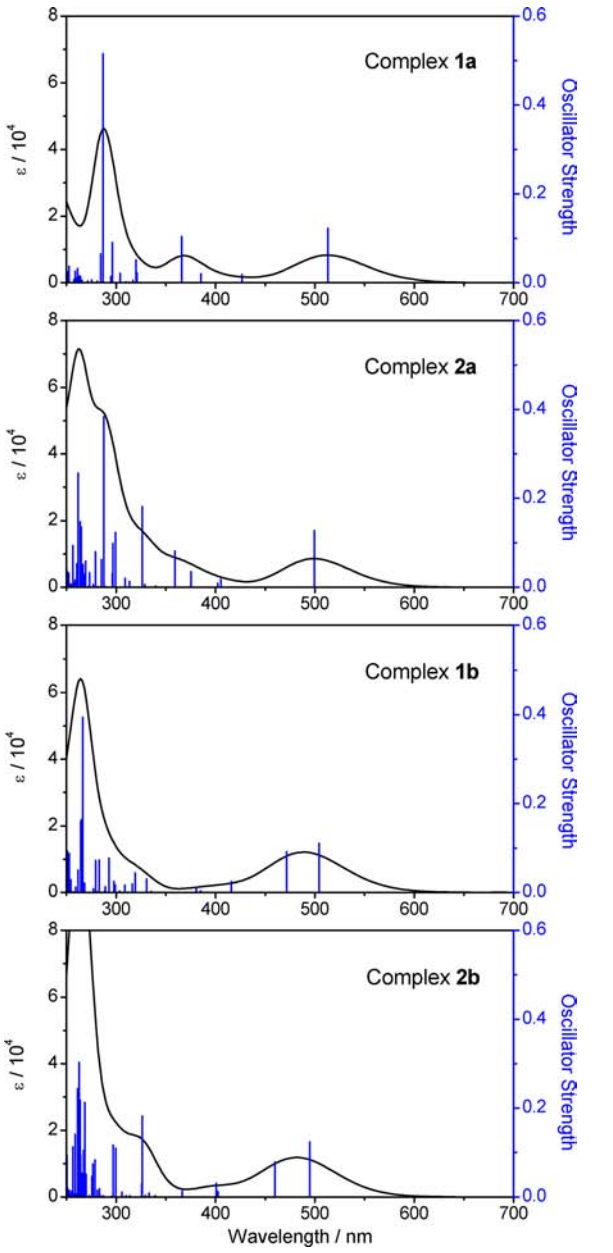

Figure 3. Calculated absorption spectra for **1a**, **2a**, **1b**, and **2b** from TD-DFT(M06 functional)/CPCM calculations. Excitation energies and oscillator strengths are shown by the blue vertical lines; spectra (in black) are convoluted with Gaussian function having full width half-maximum of 0.2 eV.

dx.doi.org/10.1021/ic202726g | Inorg. Chem. 2012, 51, 8693−8703

Table 3. Calculated Vertical Transition Energies (λ > 350 nm) for 1−2 at the TD-DFT Level[a]

		TD-DFT/CPCM calculations	
complex	experimental λ_{max}/cm^{-1} (ε_{max}/dm^3 mol^{-1} cm^{-1})	excitation energy/cm^{-1} (oscillator strength)	composition of the excited-state wave functions[b]
1a[c]	19380 (5250)	19490 (0.1224)	0.69 $\Psi_{H\rightarrow L}$
	26950 (5660)	23440 (0.0182)	0.69 $\Psi_{H-2\rightarrow L}$
		25960 (0.0205)	0.70 $\Psi_{H\rightarrow L+1}$
		27330 (0.1040)	0.68 $\Psi_{H\rightarrow L+2}$ + 0.12 $\Psi_{H-5\rightarrow L}$
1a[d]	19380 (5250)	19780 (0.1163)	0.69 $\Psi_{H\rightarrow L}$ + 0.12 $\Psi_{H-2\rightarrow L}$
	26950 (5660)	22740 (0.0197)	0.69 $\Psi_{H-2\rightarrow L}$ − 0.11 $\Psi_{H\rightarrow L}$
		25890 (0.0177)	0.69 $\Psi_{H\rightarrow L+1}$ + 0.13 $\Psi_{H\rightarrow L+2}$
		27550 (0.1188)	0.67 $\Psi_{H\rightarrow L+2}$ − 0.13 $\Psi_{H-5\rightarrow L}$ − 0.11 $\Psi_{H\rightarrow L+1}$
1b[c]	19760 (6420)	19840 (0.1104)	0.69 $\Psi_{H\rightarrow L}$ − 0.11 $\Psi_{H\rightarrow L+1}$
		21210 (0.0919)	0.69 $\Psi_{H\rightarrow L+1}$ − 0.11 $\Psi_{H\rightarrow L}$
		24050 (0.0246)	0.68 $\Psi_{H-2\rightarrow L}$
		26290 (0.0116)	0.69 $\Psi_{H-2\rightarrow L+1}$ − 0.10 $\Psi_{H-2\rightarrow L}$
1c[c]	18660 (9350)	18560 (0.2275)	0.69 $\Psi_{H\rightarrow L}$ − 0.10 $\Psi_{H\rightarrow L+2}$
	24940 (12310)	22400 (0.0450)	0.67 $\Psi_{H-2\rightarrow L}$ + 0.15 $\Psi_{H\rightarrow L+1}$
		23320 (0.1257)	0.64 $\Psi_{H\rightarrow L+1}$ + 0.25 $\Psi_{H\rightarrow L+2}$ − 0.12 $\Psi_{H-2\rightarrow L}$
		24020 (0.2230)	0.64 $\Psi_{H\rightarrow L+2}$ − 0.23 $\Psi_{H\rightarrow L+1}$ + 0.11 $\Psi_{H\rightarrow L}$ + 0.10 $\Psi_{H-2\rightarrow L}$
2a[c]	19960 (5370)	20030 (0.1272)	0.70 $\Psi_{H\rightarrow L}$
	26740 (sh, 5600)	24680 (0.0177)	0.68 $\Psi_{H-2\rightarrow L}$ − 0.10 $\Psi_{H-3\rightarrow L}$
		24870 (0.0093)	0.68 $\Psi_{H\rightarrow L+2}$ + 0.14 $\Psi_{H\rightarrow L+10}$
		26640 (0.0350)	0.70 $\Psi_{H\rightarrow L+1}$
		27850 (0.0817)	0.68 $\Psi_{H\rightarrow L+3}$ + 0.12 $\Psi_{H-6\rightarrow L}$
2b[c]	20280 (6600)	20220 (0.1238)	0.69 $\Psi_{H\rightarrow L}$ + 0.11 $\Psi_{H\rightarrow L+1}$
		21750 (0.0786)	0.69 $\Psi_{H\rightarrow L+1}$
		24840 (0.0117)	0.68 $\Psi_{H\rightarrow L+2}$ − 0.14 $\Psi_{H\rightarrow L+10}$
		24960 (0.0306)	0.68 $\Psi_{H-2\rightarrow L}$
		27290 (0.0131)	0.69 $\Psi_{H-2\rightarrow L+1}$
2c[c]	19230 (9630)	19090 (0.2479)	0.69 $\Psi_{H\rightarrow L}$
	25640 (12430)	23600 (0.0536)	0.64 $\Psi_{H-2\rightarrow L}$ − 0.25 $\Psi_{H\rightarrow L+1}$
		24210 (0.1498)	0.62 $\Psi_{H\rightarrow L+1}$ + 0.22 $\Psi_{H-2\rightarrow L}$ + 0.22 $\Psi_{H\rightarrow L+2}$
		24620 (0.1796)	0.66 $\Psi_{H\rightarrow L+2}$ − 0.17 $\Psi_{H\rightarrow L+1}$ − 0.13 $\Psi_{H-2\rightarrow L}$ − 0.10 $\Psi_{H\rightarrow L}$
		24640 (0.0099)	0.68 $\Psi_{H\rightarrow L+3}$ + 0.13 $\Psi_{H\rightarrow L+11}$

[a]Excitations with oscillator strength <5 × 10^{-3} are omitted. [b]The sum of the squares of the CI expansion coefficients is normalized to be 0.5. [c]M06 functional. [d]B3LYP functional.

moderately intense absorption bands at around 370 and 500 nm, whereas **1b** and **2b** only show moderately intense absorption at around 500 nm; the absorption profiles for **1c** and **2c** are similar to those for **1a** and **2a** except that they are slightly red-shifted. For clarity, only the calculated vertical transitions with λ > 350 nm are summarized in Table 3. Table 4 summarized the compositions of the molecular orbitals (MOs) which are involved in the lowest-energy electronic transitions in these complexes.

For **1a** and **2a** (and for **1c** and **2c**), their calculated lowest-energy dipole allowed transitions at $\lambda_{max} \approx$ 500 nm mainly originate from the HOMO → LUMO transition. Since the HOMOs have higher d(Os) contribution (20−30%) than that in LUMOs (3%), whereas the LUMOs have higher N^N contribution (40−43%) than that in HOMOs (4−7%), the transition contains $d_\pi(Os^{II})$ → N^N MLCT character. This finding parallels the spectroscopic assignment deduced from argument (III). Moreover, the contribution of C^C^C to both the HOMOs and LUMOs are not low (53−73%), revealing that the C^C^C ligands contribute significantly to both the $d_\pi(Os^{II})$ and π^*(N^N) levels.

The lowest-energy absorption bands at around 500 nm for **1b** and **2b** originate from two closely spaced vertical transitions, and this may explain why the lowest-energy absorption bands for **1b** and **2b** are not Gaussian in appearance. These two transitions are attributed to a mixing of HOMO → LUMO and HOMO → LUMO+1 transitions. The HOMO for **1b** and **2b** have higher d(Os) contribution (11−18%) than those in LUMO and LUMO+1 (<3%), and the LUMO and LUMO+1 have higher N^N contribution (26−41%) than that in HOMO (3%). It is also noted that the C^C^C has significant contribution in the HOMO, LUMO, and LUMO+1 (56−84%). Therefore the nature of the lowest-energy absorption bands for **1b** and **2b** are similar to those for **1a**, **2a**, **1c**, and **2c**, i.e. $d_\pi(Os^{II})$ → π^*(N^N) MLCT, where the $d_\pi(Os^{II})$ and π^*(N^N) levels contain significant contribution from the C^C^C ligands.

The absorptions at λ = 330−420 nm for **1a**, **2a**, **1c**, and **2c** are calculated to be attributed to the d(Os^{II}) → π^*[p(Os) + N^N] MLCT transition, where both the d(Os^{II}) and π^*[p(Os) + N^N] levels contain significant contribution from the C^C^C ligands, and the p(Os) have the correct symmetry to interact with the π system of N^N. Although **1b** and **2b** also exhibit the same type of transitions in this spectroscopic region, their oscillator strengths are calculated to be smaller compared with those for **1a**, **2a**, **1c**, and **2c**, which is because the effectiveness of the overlap between the lower/higher-energy molecular

dx.doi.org/10.1021/ic202726g | Inorg. Chem. 2012, 51, 8693−8703

Table 4. Selected Molecular Orbital Compositions (%) of 1−2

		% composition				
complex	MO	Os(s,p)	Os(d)	N^N	C^C^C	CO
1a[a]	HOMO	3.98	29.85	5.82	60.21	0.13
	LUMO	0.07	2.93	39.70	57.16	0.12
1a[b]	HOMO−2	2.60	24.66	1.50	66.11	5.11
	HOMO	5.37	36.77	7.34	50.31	0.20
	LUMO	0.61	3.10	40.03	56.08	0.16
1b[a]	HOMO	1.05	11.13	3.37	84.34	0.10
	LUMO	6.71	0.93	26.69	65.51	0.16
	LUMO+1	11.94	0.20	29.58	58.23	0.05
1c[a]	HOMO	3.63	28.05	7.27	60.94	0.10
	LUMO	2.79	2.94	40.13	53.85	0.28
2a[a]	HOMO	2.62	20.48	3.61	73.11	0.17
	LUMO	0.09	2.94	43.40	53.44	0.12
2b[a]	HOMO	2.25	17.82	3.44	76.31	0.17
	LUMO	0.33	2.27	41.03	56.22	0.13
	LUMO+1	1.11	1.37	25.79	71.68	0.05
2c[a]	HOMO	2.55	20.42	4.90	71.98	0.14
	LUMO	2.65	2.66	40.31	54.18	0.19

[a]M06 functional with CPCM (solvent = CH_3CN). [b]B3LYP functional with CPCM (solvent = CH_3CN).

orbital pairs involved in these transitions decrease when changing N^N from bpy to phen.

Emission Spectroscopy. Complexes **1**−**2** are emissive upon photoexcitation. Figure 4 depicts the excitation and

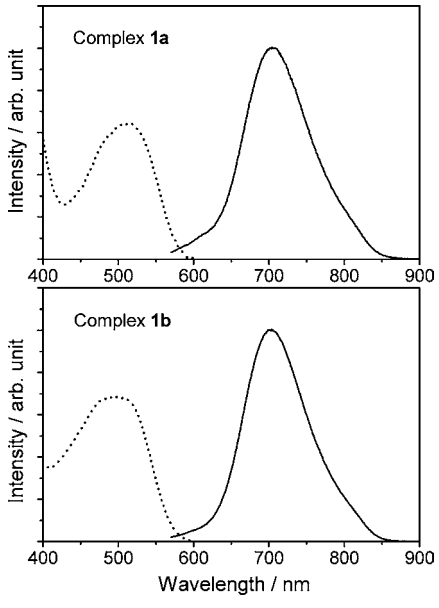

Figure 4. Excitation (dotted lines) and emission (solid lines) spectra for **1a** and **1b**.

emission spectra for **1a** and **1b** in CH_3CN at 298 K. Emission maxima of **1**−**2** range are in the red-spectral region (674−731 nm). Quantum yields (Φ) and emission lifetimes (τ) are around 10^{-4}−10^{-2} and 10^{1} μs respectively. These photophysical parameters are sensitive to the change of C^C^C and N^N, signifying that the emissive excited-state involve both the C^C^C and N^N moieties. The resemblance of the excitation profiles to the absorption spectra signify that the emissions originate from the energy dissipation of the $d_\pi(Os^{II}) \rightarrow \pi^*(N^\wedge N)$ MLCT transitions. Moreover, the emission wavelengths for all the complexes in this work are sensitive to the change of solvent. For example, all of them exhibit blue-shift (by 152−196 cm^{-1}) on emission profiles when the solvent changes from CH_3CN to CH_2Cl_2, which are comparable to those observed in $[Ru(bpy)_3]^{2+}$ and $[Os(bpy)_3]^{2+}$ (390 and 297 cm^{-1} respectively).[41a] Importantly, the emission energies for **1a** and **1b** (14200 and 14310 cm^{-1}, respectively, in CH_3CN) are blue-shifted compared with those of $[Os(bpy)_3]^{2+}$ and $[Os(phen)_3]^{2+}$ (13460 and 13890 cm^{-1} respectively in CH_3CN), and are very similar to those of $[Os(bpy)_2(CO)Cl]^+$ and $[Os(phen)_2(CO)Cl]^+$ (14120 and 14290 cm^{-1} respectively in CH_3CN).[41b] These suggest that the emissive excited state for the complexes in this work to be MLCT in nature. It is interesting to note that the emission lifetimes of these complexes are significantly longer than those of $[Os(bpy)_3]^{2+}$ and $[Os(phen)_3]^{2+}$ (60 and 262 ns respectively),[34] and are among the highest for Os(II) complexes bearing aromatic diimines.[34]

Table 5. Emission Data for Complexes 1−2 in Solution at 298 K[a,b]

complex	λ_{em}/nm	quantum yield (Φ)	lifetime (τ)/μs
	Solvent = CH_3CN		
1a	704	1.19×10^{-3}	0.62
1b	699	2.70×10^{-3}	2.42
1c	731	8.95×10^{-4}	0.70
2a	683	2.73×10^{-3}	1.07
2b	683	5.30×10^{-3}	3.67
2c	708	1.66×10^{-3}	1.25
	solvent = CH_2Cl_2		
1a	696	1.85×10^{-3}	0.91
1b	690	6.49×10^{-3}	3.98
1c	722	1.91×10^{-3}	1.06
2a	676	5.35×10^{-3}	1.53
2b	674	1.29×10^{-2}	6.09
2c	699	3.26×10^{-3}	1.93
	solvent = $(CH_3)_2CO$		
1a	706	1.06×10^{-3}	0.61
1b	704	2.94×10^{-3}	2.43
1c	731	9.52×10^{-4}	0.76
2a	685	2.61×10^{-3}	1.10
2b	682	5.78×10^{-3}	4.31
2c	707	1.87×10^{-3}	1.33
	solvent = $(CH_3)_2SO$		
1a	705	1.75×10^{-3}	0.64
1b	703	3.11×10^{-3}	2.25
1c	729	1.18×10^{-3}	0.77
2a	684	3.14×10^{-3}	1.13
2b	682	7.45×10^{-3}	4.35
2c	707	2.47×10^{-3}	1.38

[a]Concentration =3.0×10^{-5} M. [b]λ_{ex} = 450 nm.

Transient Absorption Spectroscopy and Spectroelectrochemistry. Transient absorption spectroscopic measurements (nano- to microsecond range, λ_{ex} = 355 nm) have been employed to probe the excited-state properties of **1a**, **1b**, **2a**, and **2b**; for the ease of discussion only the spectroscopic features for **2b** (the complex with the longest emission lifetime in this work) are discussed in the following, and all the arguments below also holds for other congeners in this work. The time-resolved excited-state absorption difference spectra of

dx.doi.org/10.1021/ic202726g | Inorg. Chem. 2012, 51, 8693−8703

2b are shown in Figure 5. These difference spectra clearly show the bleaching of the lowest-energy absorption band associated

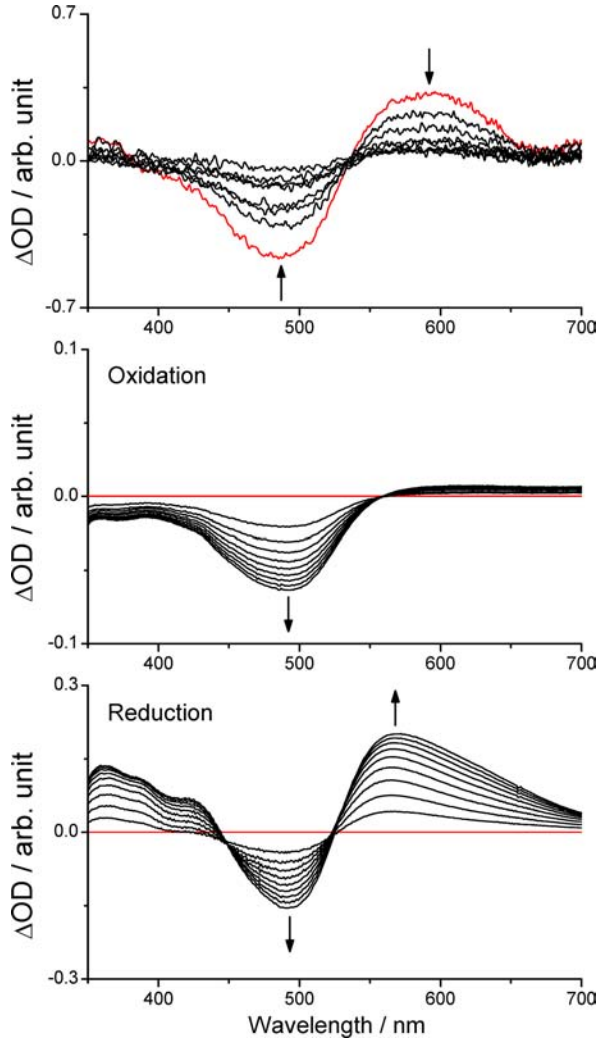

Figure 5. (Top) Transient UV−visible difference spectra for **2b** in CH_3CN at 298 K upon photoexcitation (λ_{ex} = 355 nm; 1.0 μs traces; initial trace is shown in red). (Middle and Bottom) UV−visible absorption spectra for **2b** in CH_3CN at 298 K during electrochemical oxidation and reduction (at 0.7 and −2.1 V vs $Cp_2Fe^{+/0}$; 5 s traces; initial traces are shown in red).

with **2b** (i.e., the $d_\pi(Os^{II}) \rightarrow \pi^*(N^\wedge N)$ MLCT transition): bleachings at ∼485 nm are observed in the difference spectra. On the other hand, the difference spectra also show a distinctive increase of absorption at ∼600 nm and a less intense enhancement of absorption at ∼350 nm. The transient absorption decay follows a first-order exponential kinetics, with a lifetime (3.60 μs) essentially the same as that for the emission intensity decay (3.67 μs); this suggests that the excited-state being probed by transient absorption spectroscopy in this time scale is the emissive excited-state.

A qualitative way to assign/identify these absorptions can be done with the help of spectroelectrochemical measurements. For complex in the form of [M−L] which features a M → L MLCT transition, the excited-state difference spectra for the MLCT state would be complicated by the transition characteristics of both the formally oxidized M and formally reduced L. By obtaining the absorption spectra for $[M^+-L]$ and $[M-L^-]$ generated spectroelectrochemically, the features of the excited-state difference spectra may be assigned qualitatively.[42] Electrochemical data for all the complexes are summarized in Table 6; difference spectra obtained during the electrochemical

Table 6. Electrochemical Data[a]

	$E^{1/2b}$/V vs $Cp_2Fe^{+/0}$		
complex	reduction	first oxidation	second oxidation
1a	−1.93	0.40	1.31[d]
1b	−1.95[c]	0.39	1.26[d]
1c	−1.85	0.37	1.21[d]
2a	−1.99[c]	0.50	1.35[d]
2b	−1.92[c]	0.49	1.30[d]
2c	−1.80	0.46	1.24[d]

[a]Supporting electrolyte: 0.1 M $[Bu_4N]PF_6$ in CH_3CN. [b]$E_{1/2} = (E_{pc} + E_{pa})/2$ at 298 K for reversible couples. [c]Irreversible; the recorded potential is the cathodic peak potential at scan rate of 100 mV s^{-1}. [d]Irreversible; the recorded potential is the anodic peak potential at scan rate of 100 mV s^{-1}.

oxidation and reduction for **2b** are depicted in Figure 5. Notably, reduction of **2b** results in growing absorption bands at ∼570 nm and ∼350 nm, which qualitatively correspond to the absorption features in the excited-state of **2b**. Overall, the transient absorption profiles for **2b** are fairly close to the combination of the two electrochemically generated difference spectra, and this reveals that the emissive excited-states for the complexes in this work originate from the HOMO → LUMO electronic transition, that is, $d_\pi(Os^{II}) \rightarrow \pi^*(N^\wedge N)$ MLCT transition.

GENERAL REMARKS AND CONCLUSIONS

Although there have been extensive synthetic, structural, and reactivity studies in transition-metal complexes bearing NHCs, utilizing NHCs to manipulate the photophysical properties of a [M(N^N)] core has received far less attention. In this work a series of Os(II) complexes bearing the NHC-derived tridentate C^C^C pincer ligands and aromatic diimines have been prepared. This joint experimental and theoretical investigation reveals two important findings: (1) the lowest-energy absorptions associated with these complexes mainly arise from a HOMO → LUMO transition, which is rationalized as a $d_\pi(Os^{II}) \rightarrow \pi^*(N^\wedge N)$ MLCT transition, where the C^C^C ligands contribute significantly to both the $d_\pi(Os^{II})$ and $\pi^*(N^\wedge N)$ levels; (2) these complexes are emissive with long lifetimes, and the emissive excited-states are shown to be derived from the HOMO → LUMO transitions. With the information that the contribution of C^C^C in both the HOMOs and LUMOs are not low (53−84%), it is evident that the C^C^C ligands can modulate the photophysical properties via the formation of the hybrid [Os + C^C^C] frontier orbitals. Overall, this work highlights the opportunities to use NHC-derived ligands to modulate the photophysics of a [M(N^N)] core, which would be an impact regarding the design of functional polypyridyl complexes for photonic applications.

EXPERIMENTAL SECTION

General Procedure. All reactions were performed under an argon atmosphere using standard Schlenk techniques unless otherwise stated. All reagents and solvents were used as received. The C^C^C ligand precursors, that is, benzene-bridged bisimidazolium or bisbenzimidazolium hexafluorophosphate, were prepared according to literature methods;[43] $[Os(N^\wedge N)Cl_4]$ were synthesized by a modified procedure[33] of Buckingham et al.[36] ^1H, $^{13}C\{^1H\}$, DEPT-135, $^1H-^1H$ COSY, and $^1H-^{13}C$ HSQC NMR spectra were recorded on

dx.doi.org/10.1021/ic202726g | Inorg. Chem. 2012, 51, 8693−8703

Scheme 2. Labeling Scheme for H and C Atoms in 1−2

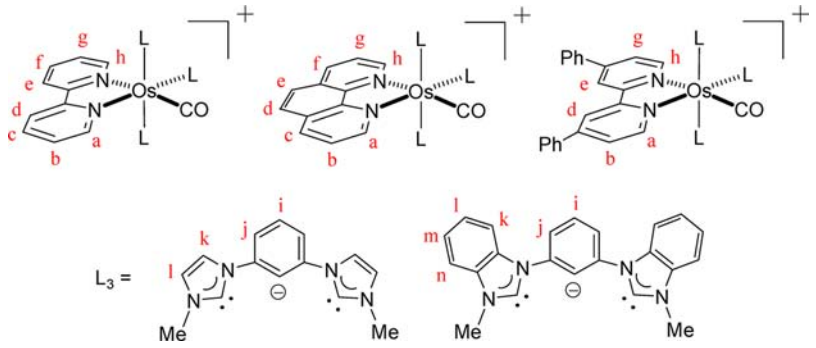

Bruker 400 DRX FT-NMR spectrometer. Peak positions were calibrated with solvent residue peaks as internal standard. Electrospray mass spectrometry was performed on a PE-SCIEX API 3000 triple quadrupole mass spectrometer. Infrared spectra were recorded as KBr plates on an Avatar 360 FTIR spectrometer. UV−visible spectra were recorded on a Shimadzu UV-1700 spectrophotometer. Elemental analyses were done on an Elementar Vario Micro Cube carbon−hydrogen−nitrogen elemental microanalyzer. Cyclic voltammetry was performed with a CH Instrument model 600C series electrochemical analyzer/workstation. All the electrochemical measurements were performed in CH_3CN solution with $[n\text{-}Bu_4N]PF_6$ (0.1 M) as supporting electrolyte at room temperature. The glassy-carbon working electrode was polished with 0.05 μm alumina on a microcloth, sonicated for 5 min in deionized water, and rinsed with CH_3CN before use. An $Ag/AgNO_3$ (0.1 M in CH_3CN) electrode was used as reference electrode, with a platinum wire as the counter electrode. All solutions were degassed with nitrogen before experiments. The $E_{1/2}$ value of the ferrocenium/ferrocene couple ($Cp_2Fe^{+/0}$) measured in the same solution was used as an internal reference. Steady-state emission spectra were obtained on a Jobin Yvon Fluorolog-3-TCSPC spectrophotometer. Sample and standard solutions were degassed with at least three freeze−pump−thaw cycles. The emission quantum yields were measured by the method of Demas and Crosby[44] with $[Ru(bpy)_3](PF_6)_2$ in degassed CH_3CN as standard (Φ_r = 0.062) and calculated by $\Phi_s = \Phi_r(B_r/B_s)(n_s/n_r)^2(D_s/D_r)$, where the subscripts s and r refer to sample and reference standard solution, respectively, n is the refractive index of the solvents, D is the integrated intensity, and Φ is the luminescence quantum yield. The quantity B is calculated by $B = 1 - 10^{-AL}$, where A is the absorbance at the excitation wavelength and L is the optical path length. Transient absorption spectra at room temperature were recorded on an Edinburgh Instruments LP920-KS spectrometer connected to an intensified charge-coupled device (ICCD). The excitation source for the transient absorption measurement was the third harmonic output (355 nm; 6−8 ns fwhm pulse width) of a Spectra-Physics Quanta-Ray Q-switched LAB-150 pulsed Nd:YAG laser (10 Hz).

[Os(C^C^C)(N^N)(CO)](PF$_6$), 1−2(PF$_6$). A mixture of [Os(N^N)Cl$_4$] (0.92 mmol) and the benzene-bridged bisimidazolium or bisbenzimidazolium hexafluorophosphate (1.01 mmol) was refluxed in ethylene glycol for 2 h. Upon cooling to room temperature, the mixture was added to saturated aqueous NH_4PF_6 solution (5 mL), and brownish purple precipitate was filtered and washed with water (2 × 5 mL). The brownish purple solid was transferred to an acetonitrile solution (50 mL) containing zinc granules (0.61 mmol). The brown mixture was refluxed for 1 h. Upon cooling to room temperature, the resultant brown solution was filtered off to remove the zinc granules and evaporated in vacuum to give brown solids. The crude product was eluted by column chromatography (basic alumina, gradual elution with CH_3CN/toluene (from 1:10 to 1:3, v/v) as eluent) as a red band. After removal of solvent, the dark red solid was recrystallized by slow diffusion of Et_2O into a CH_2Cl_2 solution to give dark red crystals.

Complex 1a(PF$_6$) (C^C^C = C^1^C^C^1; N^N = bpy). Yield: 0.49 g, 70%. Anal. Calcd for $C_{25}H_{21}N_6OOsPF_6$: C, 39.69; H, 2.80; N, 11.11. Found: C, 39.45; H, 2.76; N, 10.89. ^{1}H NMR (400 MHz, CD_3CN): δ 3.08 (s, 6H, Me), 7.04 (d, J = 2 Hz, 2H, H_l), 7.04−7.06 (m, 1H, H_g), 7.12 (d, J = 5.6 Hz, 1H, H_h), 7.37−7.39 (m, 3H, H_i + H_j), 7.59 (m, 1H, H_b), 7.75 (d, J = 2 Hz, 2H, H_k), 7.81 (m, 1H, H_f), 8.00 (m, 1H, H_c), 8.35 (d, J = 8.2 Hz, 1H, H_e), 8.43 (d, J = 8.2 Hz, 1H, H_d), 9.91 (d, J = 5.6 Hz, 1H, H_a). ^{13}C NMR (100.6 MHz, CD_3CN): δ 36.5 (Me), 109.3 (C_j), 117.4 (C_k), 123.7 (C_l), 124.2 (C_e), 125.3 (C_i), 125.5 (C_d), 126.9 (C_g), 128.4 (C_b), 135.2 (C_c), 137.8 (C_f), 148.6 (C_β of Ph), 149.8 (C_h), 150.2 (quaternary carbon of N^N), 153.2 (C_a), 154.5 (quaternary carbon of N^N), 156.9 (C_α of Ph), 172.7 (Os−C_{NHC}), 178.1 (CO). IR (KBr, cm^{-1}): ν_{CO} = 1910. ESI-MS: m/z 613.4 [M$^+$].

Complex 1b(PF$_6$) (C^C^C = C^1^C^C^1; N^N = phen). Yield: 0.43 g, 63%. Anal. Calcd for $C_{27}H_{21}N_6OOsPF_6{\cdot}CH_2Cl_2$: C, 38.85; H, 2.68; N, 9.71. Found: C, 39.11; H, 2.70 N, 9.95. ^{1}H NMR (400 MHz, CD_3CN): δ 2.87 (s, 6H, Me); 6.96 (d, J = 2.2 Hz, 2H, H_l), 7.40−7.43 (m, 5H, H_g + H_h + H_i + H_j), 7.75 (d, J = 2.2 Hz, 2H, H_k), 7.97 (dd, J = 8.1, 5.7 Hz, 1H, H_b), 8.05 (d, J = 8.8 Hz, 1H, H_e), 8.16 (d, J = 8.8 Hz, 1H, H_d), 8.37 (dd, J = 7.2, 2.4 Hz, 1H, H_f), 8.59 (dd, J = 8.1, 1.2 Hz, 1H, H_c), 10.26 (dd, J = 5.7, 1.2 Hz, 1H, H_a). ^{13}C NMR (100.6 MHz, CD_3CN): δ 36.5 (Me), 109.3 (C_j), 117.4 (C_k), 123.6 (C_l), 125.4 (C_i), 125.5 (C_h), 127.3 (C_b), 128.3 (C_e), 128.8 (C_d), 131.6, 132.7 (quaternary carbons), 134.3 (C_c), 137.3 (C_f), 146.4, 147.7, 148.8, 150.1 (quaternary carbons), 150.8 (C_g), 152.9 (C_a), 173.0 (Os−C_{NHC}), 178.4 (CO). IR (KBr, cm^{-1}): ν_{CO} = 1910. ESI-MS: m/z 635.3 [M$^+$].

Complex 1c(PF$_6$) (C^C^C = C^1^C^C^1; N^N = Ph$_2$bpy). Yield: 0.45 g, 54%. Anal. Calcd for $C_{37}H_{29}N_6OOsPF_6$: C, 48.78; H, 3.21; N, 9.23. Found: C, 48.66; H, 3.11 N, 9.28. ^{1}H NMR (400 MHz, CD_3CN): δ 3.16 (s, 6H, Me), 7.06 (d, J = 2.0 Hz, 2H, H_l), 7.33 (d, J = 5.6 Hz, 1H, H_h), 7.34 (dd, J = 5.6, 1.6 Hz, 1H, H_g), 7.40−7.44 (m, 3H, H_i + H_j), 7.49−7.77 (m, 8H, Ph), 7.78 (d, J = 2.0 Hz, 2H, H_k), 7.90 (dd, J = 5.6, 1.6 Hz, 1H, H_b), 8.02−8.04 (m, 2H, Ph), 8.75 (d, J = 1.6 Hz, 1H, H_e), 8.85 (d, J = 1.6 Hz, 1H, H_d), 9.93 (d, J = 5.6 Hz, 1H, H_a). ^{13}C NMR

dx.doi.org/10.1021/ic202726g | Inorg. Chem. 2012, 51, 8693−8703

(100.6 MHz, CD_3CN): δ 36.7 (Me), 109.3 (C_j), 117.5 (C_k), 122.1 (C_d), 123.1 (C_e), 123.8 (C_l), 124.5 (C_g), 125.4 (C_i), 126.0 (C_b), 128.0, 128.4, 130.2, 130.3 (8 carbons on Ph, resolved with $^1H-^{13}C$ HSQC NMR experiment), 130.8, 131.2 (2 carbons on Ph), 136.8, 137.3, 146.9, 148.6, 149.7 (quaternary carbons), 149.9 (C_h), 151.4 (quaternary carbon), 153.4 (C_a), 155.1, 157.6 (quaternary carbons), 172.7 (Os–C_{NHC}), 178.1 (CO). IR (KBr, cm^{-1}): ν_{CO} = 1906. ESI-MS: m/z 763.4 [M^+].

Complex 2a(PF_6) (C^C^C = C^2^C^C^2; N^N = bpy). Yield: 0.44 g, 56%. Anal. Calcd for $C_{33}H_{25}N_6OOsPF_6$: C, 46.26; H, 2.94; N, 9.81. Found: C, 46.00; H, 2.97; N, 9.72. ^1H NMR (400 MHz, CD_3CN): δ 3.32 (s, 6H, Me), 6.99–7.02 (m, 1H, H_g), 7.20 (d, J = 8.0 Hz, 1H, H_h), 7.37–7.50 (m, 6H, H_l + H_m + H_n), 7.60 (t, J = 8.0 Hz, 1H, H_i), 7.71–7.79 (m, 2H, H_b + H_f), 7.95 (d, J = 8.0, 2H, H_j), 8.10–8.14 (m, 1H, H_c), 8.24 (d, J = 8.2 Hz, 2H, H_k), 8.35 (d, J = 8.2 Hz, 1H, H_e), 8.50 (d, J = 8.2 Hz, 1H, H_d), 10.01 (d, J = 5.6 Hz, 1H, H_a). ^{13}C NMR (100.6 MHz, CD_3CN): δ 33.7 (Me), 110.7 (C_j), 112.1 (C_l/C_m), 112.3 (C_k), 124.4 (C_e), 124.5, 125.0 (C_l/Cm + Cn), 125.7 (C_d), 126.0 (C_i), 127.2 (C_g), 129.0 (C_b), 133.1 (quaternary carbon), 136.2 (C_c), 136.9 (quaternary carbon), 138.2 (C_f), 149.3 (quaternary carbon), 150.3 (C_h), 150.6 (quaternary carbon), 153.5 (C_a), 155.0 (quaternary carbon), 157.0 (C_α of Ph), 178.6 (CO), 185.1 (Os–C_{NHC}). IR (KBr, cm^{-1}): ν_{CO} = 1924. ESI-MS: m/z 713.5 [M^+].

Complex 2b(PF_6) (C^C^C = C^2^C^C^2; N^N = phen). Yield: 0.37 g, 48%. Anal. Calcd for $C_{35}H_{25}N_6OOsPF_6{\cdot}CH_2Cl_2$: C, 44.77; H, 2.82; N, 8.70. Found: C, 44.53; H, 3.00 N, 8.85. ^1H NMR (400 MHz, CD_3CN): δ 3.12 (s, 6H, Me), 7.34–7.40 (m, 5H, H_h + H_l + H_n), 7.43–7.50 (m, 3H, H_g + H_m), 7.64 (t, J = 8.0 Hz, 1H, H_i), 7.99 (d, J = 8.0 Hz, 2H, H_j), 8.04 (d, J = 8.9 Hz, 1H, H_e), 8.10 (dd, J = 8.3, 5.4 Hz, 1H, H_b), 8.19 (d, J = 8.9 Hz, 1H, H_d), 8.25 (d, J = 8.4 Hz, 2H, H_k), 8.33 (dd, J = 8.2, 1.2, 1H, H_f), 8.70 (dd, J = 8.3, 1.2, 1H, H_c), 10.36 (dd, J = 5.4, 1.2, 1H, H_a). ^{13}C NMR (100.6 MHz, CD_3CN): δ 33.7 (Me), 110.8 (C_j), 112.0 (C_h/C_l/C_m/C_n), 112.3 (C_k), 124.3, 124.9, 125.8 (3 carbons from C_h/C_l/C_m/C_n), 126.2 (C_i), 127.7 (C_b), 128.6 (C_e), 128.8 (C_d), 131.9, 132.8, 133.1 (quaternary carbons), 135.3 (C_c), 136.8 (quaternary carbon), 137.7 (C_f), 146.7, 148.0, 149.5, 150.5 (quaternary carbons), 151.4 (C_g), 153.3 (C_a), 179.0 (CO), 185.3 (Os–C_{NHC}). IR (KBr, cm^{-1}): ν_{CO} = 1924. ESI-MS: m/z 737.2 [M^+].

Complex 2c(PF_6) (C^C^C = C^2^C^C^2; N^N = Ph_2bpy). Yield: 0.30 g, 32%. Anal. Calcd for $C_{45}H_{33}N_6OOsPF_6$: C, 53.45; H, 3.29; N, 8.32. Found: C, 53.60; H, 3.34 N, 8.23. ^1H NMR (400 MHz, CD_3CN): δ 3.41 (s, 6H, Me), 7.21 (d, J = 5.6 Hz, 1H, H_h), 7.28 (dd, J = 5.6, 1.6 Hz, 1H, H_g), 7.38–7.70 (m, 15H: 8H, Ph; 2H, H_k/H_n; 4H, H_l + H_m; 1H, H_i), 7.98 (d, J = 8.0 Hz, 2H, H_j), 8.04 (dd, J = 5.6, 1.6 Hz, 1H, H_b), 8.08 (m, 2H, Ph), 8.26 (m, 2H, H_k/H_n), 8.75 (d, J = 1.6 Hz, 1H, H_e), 8.92 (d, J = 1.6 Hz, 1H, H_d), 10.03 (d, J = 5.6 Hz, 1H, H_a). ^{13}C NMR (100.6 MHz, CD_3CN): δ 33.9 (Me), 110.8 (C_j), 112.2 (C_k/C_n), 112.3 (C_k/C_n), 122.4 (C_e), 123.4 (C_d), 124.4 (C_l/C_m), 124.8 (C_g), 125.0 (C_i), 126.1 (C_l/C_m), 126.6 (C_b), 128.2, 128.4, 130.2, 130.4 (8 carbons on Ph, resolved with $^1H-^{13}C$ HSQC NMR experiment), 131.0, 131.2 (2 carbons on Ph), 133.1, 137.0, 137.1, 147.8, 149.4, 150.0 (quaternary carbons), 150.4 (C_h), 150.7, 153.1 (quaternary carbons), 153.6 (C_a), 155.5, 157.6 (quaternary carbons), 176.2 (CO), 185.0 (Os–C_{NHC}). IR (KBr, cm^{-1}): ν_{CO} = 1927. ESI-MS: m/z 863.9 [M^+].

X-ray Crystallography. X-ray diffraction data for **1a**(PF_6), **1b**(PF_6)·CH_2Cl_2, and **2a**(PF_6)·CH_2Cl_2·Et_2O were collected on an Oxford Diffraction Gemini S Ultra X-ray single crystal diffractometer with Cu Kα radiation (λ = 1.54178 Å) at 133 K. The data were processed using CrysAlis.[45] The structures were solved by Patterson and Fourier methods and refined by full-matrix least-squares based on F^2 with program SHELXS-97 and SHELXL-97[46] within WinGX.[47] All non-hydrogen atoms were refined anisotropically in the final stage of least-squares refinement. The positions of H atoms were calculated based on riding mode with thermal parameters equal to 1.2 times that of the associated C atoms. Disorder of the PF_6^- and solvent molecules Et_2O in **2a**(PF_6)·CH_2Cl_2·Et_2O were observed. Split models were applied to the PF_6^-. The highly disordered Et_2O were modeled to be a moiety containing four carbon atoms and one oxygen atom, and no hydrogen atoms were assigned.

Computational Methodology. DFT calculations were performed on **1**–**2**. Their electronic ground states were optimized with *Cs* symmetry imposed using the hybrid functional M06 by Truhlar and Zhao.[38] The M06 functional was employed because it is a functional parametrized for transition metals, and had been demonstrated to give higher accuracy than other hybrid functionals in transition metal and organometallic chemistry.[38] The ECP60MDF pseudopotential was employed for the Os atoms with the correlation consistent cc-pVTZ-PP basis set of Peterson et al.[48] The 6-311+G* basis set was employed for C, H, N, and O atoms.[49] Tight SCF convergence (10^{-8} au) was used for all calculations. Frequency calculations were performed on the optimized structures for **1a** and **1b**. As no imaginary vibrational frequencies were encountered, their optimized stationary points were confirmed to be local minima. The vibrational frequencies for **1c**, **2a**, **2b**, and **2c** were not calculated due to computational limitation. The vertical transition energies for these complexes in CH_3CN were computed at their respective gas-phase optimized ground-state geometries using time-dependent-DFT (TD-DFT) method with the same density functional and basis sets in the geometry optimizations. Meanwhile, a TD-DFT calculation using the B3LYP functional[39] has also been performed on **1a** (using the M06 optimized geometry) for comparison. The conductor polarizable continuum model (CPCM)[40] was used to account for solvent effects upon the electronic transition. All the calculations were performed using the Gaussian 09 program package (revision B.01).[50]

■ ASSOCIATED CONTENT

Ⓢ Supporting Information

Calculated absorption spectrum for **1a** from TD-DFT(B3LYP functional)/CPCM calculation; optimized geometries for **1**–**2**, molecular orbital compositions for **1**–**2**, which are of spectroscopic importance, and crystallographic information files (CIF). This material is available free of charge via the Internet at http://pubs.acs.org.

■ AUTHOR INFORMATION

Corresponding Author

*acywong@cityu.edu.hk.

Notes

The authors declare no competing financial interest.

■ ACKNOWLEDGMENTS

The work described in this paper was supported by grants from the Hong Kong Research Grants Council (Project No. CityU 103911) and City University of Hong Kong (Project No.

7002757), and the Special Equipment Grant from the University Grants Committee of Hong Kong (SEG_CityU02). We are grateful to Dr. Shek-Man Yiu for X-ray diffraction data collection, and Dr. Chun-Yu Ho for giving constructive comments on NMR experiments.

REFERENCES

(1) Kalyanasundaram, K. *Coord. Chem. Rev.* **1982**, *46*, 159.
(2) Balzani, V.; Sabbatini, N.; Scandola, F. *Chem. Rev.* **1986**, *86*, 319.
(3) Juris, A.; Balzani, V.; Barigelletti, F.; Campagna, S.; Belser, P.; von Zelewsky, A. *Coord. Chem. Rev.* **1988**, *84*, 85.
(4) Meyer, T. J. *Acc. Chem. Res.* **1989**, *22*, 163.
(5) Balzani, V.; Barigelletti, F.; De Cola, L. *Top. Curr. Chem.* **1990**, *158*, 31.
(6) Sauvage, J.-P.; Collin, J.-P.; Chambron, J.-C.; Guillerez, S.; Coudret, C.; Balzani, V.; Barigelletti, F.; De Cola, L.; Flamigni, L. *Chem. Rev.* **1994**, *94*, 993.
(7) Balzani, V.; Juris, A.; Venturi, M.; Campagna, S.; Serroni, S. *Chem. Rev.* **1996**, *96*, 759.
(8) de Silva, A. P.; Gunaratne, H. Q. N.; Gunnlaugsson, T.; Huxley, A. J. M.; McCoy, C. P.; Rademacher, J. T.; Rice, T. E. *Chem. Rev.* **1997**, *97*, 1515.
(9) Dixon, I. M.; Collin, J.-P.; Sauvage, J.-P.; Flamigni, L.; Encinas, S.; Barigelletti, F. *Chem. Soc. Rev.* **2000**, *29*, 385.
(10) De Cola, L.; Belser, P.; von Zelewsky, A.; Vögtle, F. *Inorg. Chim. Acta* **2007**, *360*, 775.
(11) Campagna, S.; Puntoriero, F.; Nastasi, F.; Bergamini, G.; Balzani, V. *Top. Curr. Chem.* **2007**, *280*, 117.
(12) Flamigni, L.; Collin, J.-P.; Sauvage, J.-P. *Acc. Chem. Res.* **2008**, *41*, 857.
(13) Lainé, P. P.; Campagna, S.; Loiseau, F. *Coord. Chem. Rev.* **2008**, *252*, 2552.
(14) For reviews, see: (a) Balzani., V.; Juris, A. *Coord. Chem. Rev.* **2001**, *211*, 97. (b) Yersin, H.; Kratzer, C. *Coord. Chem. Rev.* **2002**, *229*, 75. (c) Polo, A.-S.; Itokazu, M. K.; Iha, N. Y. M. *Coord. Chem. Rev.* **2004**, *248*, 1343. (d) Kumaresan, D.; Shankar, K.; Vaidya, S.; Schmehl, R. H. *Top. Curr. Chem.* **2007**, *281*, 101.
(15) For recent publications, see: (a) Nazeeruddin, M. K.; Pechy, P.; Renouard, T.; Zakeeruddin, S. M.; Humphry-Baker, R.; Comte, P.; Liska, R.; Cevey, L.; Costa, E.; Shklover, V.; Spiccia, L.; Deacon, G. B.; Bignozzi, C. A.; Grätzel, M. *J. Am. Chem. Soc.* **2001**, *123*, 1613. (b) Grätzel, M. *Nature* **2001**, *414*, 338. (c) Grätzel, M. *Inorg. Chem.* **2005**, *44*, 6841.
(16) For reviews, see: (a) Lowry, M. S.; Bernhard, S. *Chem.—Eur. J.* **2006**, *12*, 7970. (b) Chou, P.-T.; Chi, Y. *Eur. J. Inorg. Chem.* **2006**, 3319.
(17) For recent publications, see: (a) Adachi, C.; Kwong, R. C.; Djurovich, P.; Adamovich, V.; Baldo, M.-A.; Thompson, M. E.; Forrest, S. R. *Appl. Phys. Lett.* **2001**, *79*, 2082. (b) Lamansky, S.; Djurovich, P.; Murphy, D.; Abdel-Razzaq, F.; Lee, H.-E.; Adachi, C.; Burrows, P. E.; Forrest, S. R.; Thompson, M. E. *J. Am. Chem. Soc.* **2001**, *123*, 4304. (c) Carlson, B.; Phelan, G. D.; Kaminsky, W.; Dalton, L.; Jiang, X.; Liu, S.; Jen, A. K.-Y. *J. Am. Chem. Soc.* **2002**, *124*, 14162. (d) Chen, Y.-L.; Lee, S.-W.; Chi, Y.; Hwang, K.-C.; Kumar, S.-B.; Hu, Y.-H.; Cheng, Y.-M.; Chou, P.-T.; Peng, S.-M.; Lee, G.-H.; Yeh, S.-J.; Chen, C.-T. *Inorg. Chem.* **2005**, *44*, 4287. (e) Walsh, P. J.; Lundin, N. J.; Gordon, K. C.; Kim, J.-Y.; Lee, C.-H. *Opt. Mater.* **2009**, *31*, 1525.
(18) Bonnet, S.; Collin, J.-P.; Koizumi, M.; Mobian, P.; Sauvage, J.-P. *Adv. Mater.* **2006**, *18*, 1239.
(19) (a) Erkkila, K. E.; Odom, D. T.; Barton, J. K. *Chem. Rev.* **1999**, *99*, 2777. (b) Ji, L.-N.; Zou, X.-H.; Liu, J.-G. *Coord. Chem. Rev.* **2001**, *216–217*, 513. (c) Zeglis, B. M.; Pierre, V. C.; Barton, J. K. *Chem Commun.* **2007**, 4565.
(20) Lees, A. J. *Chem. Rev.* **1987**, *87*, 711.
(21) Maestri, M.; Balzani, V.; Deuschel-Cornioley, C.; von Zelewsky, A. *Adv. Photochem.* **1992**, *17*, 1.
(22) Djukic, J.-P.; Sortais, J.-B.; Barloy, L.; Pfeffer, M. *Eur. J. Inorg. Chem.* **2009**, 817.
(23) Beley, M.; Chodorowski, S.; Collin, J.-P.; Sauvage, J.-P.; Flamigni, L.; Barigelletti, F. *Inorg. Chem.* **1994**, *33*, 2543.
(24) Yu, J.-K.; Hu, Y.-H.; Cheng, Y.-M.; Chou, P.-T.; Peng, S.-M.; Lee, G.-H.; Carty, A.-J.; Tung, Y.-L.; Lee, S.-W.; Chi, Y.; Liu, C.-S. *Chem.—Eur. J.* **2004**, *10*, 6255.
(25) Arduengo, A. J.; Harlow, R. L.; Kline, M. *J. Am. Chem. Soc.* **1991**, *113*, 361.
(26) For reviews, see: (a) Herrmann, W. A. *Angew. Chem., Int. Ed.* **2002**, *41*, 1290. (b) Perry, M. C.; Burgess, K. *Tetrahedron: Asymmetry* **2003**, *14*, 951. (c) César, V.; Bellemin-Laponnaz, S.; Gade, L. H. *Chem. Soc. Rev.* **2004**, *33*, 619. (d) Zinn, F. K.; Viciu, M. S.; Nolan, S. P. *Annu. Rep. Prog. Chem., Sect. B* **2004**, *100*, 231. (e) Crudden, C. M.; Allen, D. P. *Coord. Chem. Rev.* **2004**, *248*, 2247. (f) Crabtree, R. H. *J. Organomet. Chem.* **2005**, *690*, 5451. (g) Hahn, F. E. *Angew. Chem., Int. Ed.* **2006**, *45*, 1348. (h) Díez-González, S.; Nolan, S. P. *Coord. Chem. Rev.* **2007**, *251*, 874. (i) Schuster, O.; Yang, L.; Raubenheimer, H. G.; Albrecht, M. *Chem. Rev.* **2009**, *109*, 3445. (j) Lin, J. C. Y.; Huang, R. T. W.; Lee, C. S.; Bhattacharyya, A.; Hwang, W. S.; Lin, I. J. B. *Chem. Rev.* **2009**, *109*, 3561. (k) Díez-González, S.; Marion, N.; Nolan, S. P. *Chem. Rev.* **2009**, *109*, 3612. (l) Poyatos, M.; Mata, J. A.; Peris, E. *Chem. Rev.* **2009**, *109*, 3677. (m) Samojłowicz, C.; Bieniek, M.; Grela, K. *Chem. Rev.* **2009**, *109*, 3708. (n) Alcaide, B.; Almendros, P.; Luna, A. *Chem. Rev.* **2009**, *109*, 3817. (o) Clavier, H.; Nolan, S. P. *Chem. Commun.* **2010**, *46*, 841.
(27) (a) Colacino, E.; Martinez, J.; Lamaty, F. *Coord. Chem. Rev.* **2007**, *251*, 726. (b) Mata, J. A.; Poyatos, M.; Peris, E. *Coord. Chem. Rev.* **2007**, *251*, 841. (c) Jacobsen, H.; Correa, A.; Poater, A.; Costabile, C.; Cavallo, L. *Coord. Chem. Rev.* **2009**, *231*, 687.
(28) (a) Sajoto, T.; Djurovich, P. I.; Tamayo, A.; Yousufuddin, M.; Bau, R.; Thompson, M. E.; Holmes, R. J.; Forrest, S. R. *Inorg. Chem.* **2005**, *44*, 7992. (b) Chang, C. F.; Cheng, Y. M.; Chi, Y.; Chiu, Y. C.; Lin, C. C.; Lee., G. H.; Chou, P. T.; Chen, C. C.; Chang, C. H.; Wu, C. C. *Angew. Chem., Int. Ed.* **2008**, *47*, 4542. (c) Tennyson, A. G.; Rosen, E. L.; Collins, M. S.; Lynch, V. M.; Bielawski, C. W. *Inorg. Chem.* **2009**, *48*, 6924.
(29) (a) Wang, H. M. J.; Chen, C. Y. L.; Lin, I. J. B. *Organometallics* **1999**, *18*, 1216. (b) Catalano, V. J.; Malwitz, M. A. *Inorg. Chem.* **2003**, *42*, 5483. (c) Catalano, V. J.; Malwitz, M. A.; Etogo, A. O. *Inorg. Chem.* **2004**, *43*, 5714. (d) Catalano, V. J.; Moore, A. L. *Inorg. Chem.* **2005**, *44*, 6558. (e) Barnard, P. J.; Wedlock, L. E.; Baker, M. V.; Berners-Price, S. J.; Joyce, D. A.; Skelton, B. W.; Steer, J. H. *Angew. Chem., Int. Ed.* **2006**, *45*, 5966. (f) Zhou, Y.; Chen, W. *Organometallics* **2007**, *26*, 2742. (g) Liu, B.; Chen, W.; Jin, S. *Organometallics* **2007**, *26*, 3660. (h) Ray, L.; Shaikh, M. M.; Ghosh, P. *Inorg. Chem.* **2008**, *47*, 230. (i) Strasser, C. E.; Catalano, V. J. *J. Am. Chem. Soc.* **2010**, *132*, 10009. (j) Catalano, V. J.; Munro, L. B.; Strasser, C. E.; Samin, A. F. *Inorg. Chem.* **2011**, *50*, 8465.
(30) (a) Unger, Y.; Meyer, D.; Molt, O.; Schildknecht, C.; Münster, I.; Wagenblast, G.; Strassner, T. *Angew. Chem., Int. Ed.* **2010**, *49*, 10214. (b) Lee, C.-S.; Sabiah, S.; Wang, J.-C.; Hwang, W.-S.; Lin, I. J. B. *Organometallics* **2010**, *29*, 286. (c) Zhang, Y.; Garg, J. A.; Michelin, C.; Fox, T.; Blacque, O.; Venkatesan, K. *Inorg. Chem.* **2011**, *50*, 1220. (d) Lee, C. S.; Zhuang, R. R.; Sabiah, S.; Wang, J. C.; Hwang, W. S.; Lin, I. J. B. *Organometallics* **2011**, *30*, 3897.
(31) (a) Son, S. U.; Park, K. H.; Lee, Y. S.; Kim, B. Y.; Choi, C. H.; Lah, M. S.; Jang, Y. H.; Jang, D. J.; Chung, Y. K. *Inorg. Chem.* **2004**, *43*, 6896. (b) Park, H. J.; Kim, K. H.; Choi, S. Y.; Kim, H. M.; Lee, W. I.; Kang, Y. K.; Chung, Y. K. *Inorg. Chem.* **2010**, *49*, 7340.
(32) (a) Wong, C.-Y.; Lai, L.-M.; Lam, C.-Y.; Zhu, N. *Organometallics* **2008**, *27*, 5806. (b) Wong, C.-Y.; Lai, L.-M.; Leung, H.-F.; Wong, S.-H. *Organometallics* **2009**, *28*, 3537. (c) Wong, C.-Y.; Lai, L.-M.; Pat, P.-K. *Organometallics* **2009**, *28*, 5656. (d) Wong, C.-Y.; Lai, L.-M.; Chan, S.-C.; Tai, L.-H. *Organometallics* **2010**, *29*, 6259. (e) Chan, S.-C.; Pat, P.-K.; Lau, T.-C.; Wong, C.-Y. *Organometallics* **2011**, *30*, 1311. (f) Chan, S.-C.; Cheung, H.-Y.; Wong, C.-Y. *Inorg. Chem.* **2011**, *50*, 11636.

(33) Wong, C.-Y.; Lai, L.-M.; Pat, P.-K.; Chung, L.-H. *Organometallics* **2010**, *29*, 2533.
(34) Johnson, S. R.; Westmoreland, T. D.; Caspar, J. V.; Barqawi, K. R.; Meyer, T. J. *Inorg. Chem.* **1988**, *27*, 3195.
(35) (a) Levison, J. J.; Robinson, S. D. *J. Chem. Soc. A* **1970**, 2947. (b) Bhattacharyya, R.; Drago, R. S.; Abboud, K. A. *Inorg. Chem.* **1997**, *36*, 2913. (c) Poyatos, M.; Mata, J. A.; Falomir, E.; Crabtree, R. H.; Peris, E. *Organometallics* **2003**, *22*, 1110.
(36) Buckingham, D. A.; Dwyer, F. P.; Goodwin, H. A.; Sargeson, A. M. *Aust. J. Chem.* **1964**, *17*, 315.
(37) (a) Castarlenas, R.; Esteruelas, M. A.; Oñate, E. *Organometallics* **2007**, *26*, 2129. (b) Baya, M.; Eguillor, B.; Esteruelas, M. A.; Oliván, M.; Oñate, E. *Organometallics* **2007**, *26*, 6556. (c) Eguillor, B.; Esteruelas, M. A.; Oliván, M.; Puerta, M. *Organometallics* **2008**, *27*, 445. (d) Castarlenas, R.; Esteruelas, M. A.; Lalrempuia, R.; Oliván, M.; Oñate, E. *Organometallics* **2008**, *27*, 795. (e) Castarlenas, R.; Esteruelas, M. A.; Oñate, E. *Organometallics* **2008**, *27*, 3240. (f) Cooke, C. E.; Jennings, M. C.; Katz, M. J.; Pomeroy, R. K.; Clyburne, J. A. C. *Organometallics* **2008**, *27*, 5777.
(38) (a) Zhao, Y.; Truhlar, D. G. *Acc. Chem. Res.* **2008**, *41*, 157. (b) Zhao, Y.; Truhlar, D. G. *Theor. Chem. Acc.* **2008**, *120*, 215.
(39) (a) Becke, A. D. *J. Chem. Phys.* **1993**, *98*, 5648. (b) Lee, C.; Yang, W.; Parr, R. G. *Phys. Rev. B.* **1988**, *37*, 785.
(40) Barone, V.; Cossi, M. *J. Phys. Chem. A* **1998**, *102*, 1995.
(41) (a) For $Ru(bpy)_3]^{2+}$: Durham, B.; Caspar, J. V.; Nagle, J. K.; Meyer, T. J. *J. Am. Chem. Soc.* **1982**, *104*, 4803. For $[Os(bpy)_3]^{2+}$: data were measured in this work. (b) Kober, E. M.; Caspar, J. V.; Lumpkin, R. S.; Meyer, T. J. *J. Phys. Chem.* **1986**, *90*, 3722.
(42) (a) Braterman, P. S.; Song, J.-I.; Peacock, R. D. *Spectrochim. Acta* **1992**, *48*, 899. (b) Curtright, A. E.; McCusker, J. K. *J. Phys. Chem. A* **1999**, *103*, 7032. (c) Damrauer, N. H.; McCusker, J. K. *J. Phys. Chem. A* **1999**, *103*, 8440.
(43) Vargas, V. C.; Rubio, R. J.; Hollis, T. K.; Salcido, M. E. *Org. Lett.* **2003**, *5*, 4847.
(44) Demas, J. N.; Crosby, G. A. *J. Phys. Chem.* **1971**, *75*, 991.
(45) *CrysAlis*, version 1.171.31.8; Oxford Diffraction Ltd., 2007.
(46) Sheldrick, G. M. *SHELXS-97 and SHELXL-97, Program for Crystal Structure Solution and Refinements*; University of Göttingen: Göttingen, Germany, 1997.
(47) Farrugia, L. J. *J. Appl. Crystallogr.* **1999**, *32*, 837.
(48) Figgen, D.; Peterson, K. A.; Dolg, M.; Stoll, H. *J. Chem. Phys.* **2009**, *130*, 164108.
(49) Krishnan, R.; Binkley, J. S.; Seeger, R.; Pople, J. A. *J. Chem. Phys.* **1980**, *72*, 650.
(50) Frisch, M. J.; Trucks, G. W.; Schlegel, H. B.; Scuseria, G. E.; Robb, M. A.; Cheeseman, J. R.; Scalmani, G.; Barone, V.; Mennucci, B.; Petersson, G. A.; Nakatsuji, H.; Caricato, M.; Li, X.; Hratchian, H. P.; Izmaylov, A. F.; Bloino, J.; Zheng, G.; Sonnenberg, J. L.; Hada, M.; Ehara, M.; Toyota, K.; Fukuda, R.; Hasegawa, J.; Ishida, M.; Nakajima, T.; Honda, Y.; Kitao, O.; Nakai, H.; Vreven, T.; Montgomery, Jr., J. A.; Peralta, J. E.; Ogliaro, F.; Bearpark, M.; Heyd, J. J.; Brothers, E.; Kudin, K. N.; Staroverov, V. N.; Kobayashi, R.; Normand, J.; Raghavachari, K.; Rendell, A.; Burant, J. C.; Iyengar, S. S.; Tomasi, J.; Cossi, M.; Rega, N.; Millam, N. J.; Klene, M.; Knox, J. E.; Cross, J. B.; Bakken, V.; Adamo, C.; Jaramillo, J.; Gomperts, R.; Stratmann, R. E.; Yazyev, O.; Austin, A. J.; Cammi, R.; Pomelli, C.; Ochterski, J. W.; Martin, R. L.; Morokuma, K.; Zakrzewski, V. G.; Voth, G. A.; Salvador, P.; Dannenberg, J. J.; Dapprich, S.; Daniels, A. D.; Farkas, Ö.; Foresman, J. B.; Ortiz, J. V.; Cioslowski, J.; Fox, D. J. *Gaussian 09*, revision B.01; Gaussian, Inc.: Wallingford CT, 2009.